Disease of the Gallbladder and Biliary Tree

5

Jeong Min Lee and Daniel T. Boll

Learning Objectives

- To discuss typical imaging features of common cholangiopathies.
- To discuss the imaging diagnosis of premalignant tumors of the gallbladder and bile duct.
- To explain the classical and emerging classification systems of cholangiocarcinoma.
- To discuss the strengths and weaknesses of imaging modalities and the role of multimodality and multiparametric approaches in the diagnostic work-up of biliary malignancies.

5.1 Biliary Tract

Jeong Min Lee, M.D.

5.1.1 Congenital Biliary Anomalies

5.1.1.1 Choledochal Cyst

Choledochal cyst involves congenital cystic dilatation of any portion of the extrahepatic bile ducts, and most choledochal cysts are diagnosed in childhood; however, up to 20% of cysts manifest in adults. It is classified based on the spectrum of morphologic changes in the bile ducts. The most common classification scheme is the Todani modification of the Alonso-Lej classification.

Todani type I—single cystic dilatation of the extrahepatic bile duct (EBD).
Todani Type II—true diverticula of the EBD.
Todani Type III—choledochocele or ectasia of an intramural EBD segment.
Todani Type IV—multiple and can have both intrahepatic and extrahepatic components.
Todani Type V (Caroli disease)—cystic dilatation of the intrahepatic bile ducts (IBDs).

Complications of choledochal cysts in adults include rupture with bile peritonitis, stone formation, cholangitis, liver abscess, and cholangiocarcinoma (CC). CC arising in a choledochal cysts appears as an intracystic soft tissue density mass or irregular thickening of the cyst wall [1].

5.1.2 Choledocholithiasis

Regardless of whether bile duct dilatation is present, the visible ducts should be scrutinized to identify and characterize filling defects, the vast majority of which represent stones [2]. Detectability of a bile duct stone on CT depends on the calcium content and requires precontrast CT. Depending on the composition, stones may show soft tissue attenuation, near-water attenuation, or fat attenuation with peripheral calcification. Stones are manifested as a signal void on T2-weighted imaging or MRCP (Fig. 5.1). On T1-weighted imaging, cholesterol stones are generally iso- or hypointense, while pigment stones are hyperintense due to the presence of metal ions. ERCP is highly accurate for the detection of small choledocholithiasis and also provides access for therapeutic intervention.

J. M. Lee, M.D.
Department of Radiology, Seoul National University Hospital, Seoul, Republic of Korea
e-mail: jmsh@snu.ac.kr

D. T. Boll, M.D. (✉)
Department of Radiology and Nuclear Medicine, University Hospital of Basel, Basel, BS, Switzerland
e-mail: Daniel.Boll@usb.ch

J. Hodler et al. (eds.), *Diseases of the Abdomen and Pelvis 2018–2021*, IDKD Springer Series,
https://doi.org/10.1007/978-3-319-75019-4_5

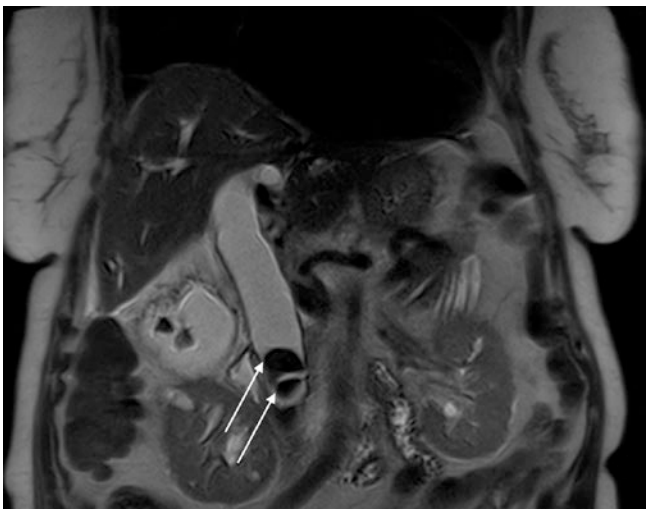

Fig. 5.1 70-year-old male patient with choledocholithiasis (arrows) in the retropancreatic portion of the hepatocholedochal duct as seen on coronal T2-weighted breathheld MR sequences. Note the distention of the DHC and further concrements in the chronically inflamed gallbladder

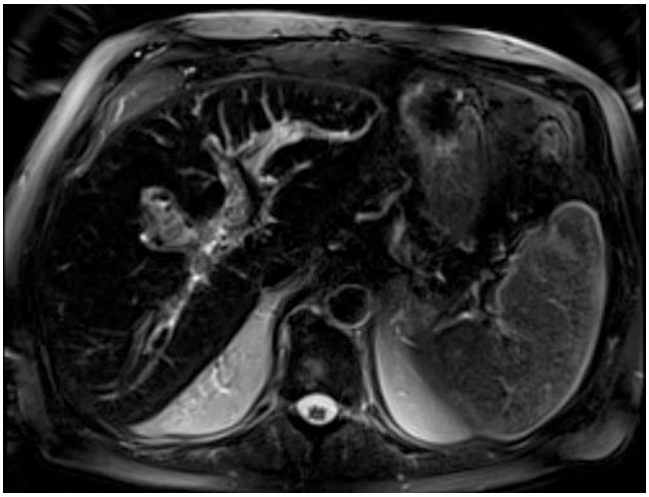

Fig. 5.2 25-year-old male patient post liver transplant with chronic cholangitis showing multiple concrements and sludge in the intrahepatic biliary system with widening of the biliary ducts and surrounding inflammatory changes as seen on axial T2-weighted fat-saturated MR images

5.1.3 Inflammatory Disorders (Cholangitis)

5.1.3.1 Suppurative Cholangitis

Acute bacterial cholangitis is a potentially life-threatening infection, usually arising in the setting of bile duct obstruction, with ensuing bacterial contamination, stagnant bile, and increased biliary pressures. Choledocholithiasis accounts for up to 80% of cases of acute cholangitis (Fig. 5.2). CT or MRI shows diffuse, concentric wall thickening of the bile duct with associated periductal edema and mural enhancement, with or without pneumobilia [3]. Marked inhomogeneous parenchymal enhancement in the arterial is frequently present in patients with acute suppurative cholangitis [4].

5.1.3.2 Recurrent Pyogenic Cholangitis

Recurrent pyogenic cholangitis is characterized by stenosis or strictures of the peripheral ducts, with decreased branching and abrupt tapering ("arrowhead appearance") associated with disproportionate dilatation of the central and extrahepatic bile ducts [5]. Sonography, CT, and MRCP not only allow the correct diagnosis to be made but also serve as a vital road map for subsequent intervention by illustrating the location and extent of disease [6]. MRCP findings of RPC include IBD or EBD stones, multiple strictures of IBD, short-segment focal EBD stricture, localized dilatation of lobar or segmental bile ducts with a predilection for the lateral segment of the left lobe and the posterior segment of the right lobe, bile duct wall thickening, abrupt tapering, and decreased arborization of the IBDs [7]. CC associated with RPC most frequently occurs in segments with a high stone burden or at atrophied segments, and suggestive imaging features of CC development include progressive atrophy of affected hepatic segments or lobes and narrowing or obliteration of the portal vein [8, 9].

5.1.3.3 Primary Sclerosing Cholangitis

PSC is a progressive cholestatic disease characterized by inflammation and fibrosis of the bile duct which is commonly associated with inflammatory bowel disease [10]. Diagnosis of primary sclerosing cholangitis can be made by typical cholangiographic findings and the exclusion of secondary causes. The typical cholangiographic features include diffuse, multifocal short-segmental strictures and mild dilatation in the intrahepatic and extrahepatic bile ducts alternating with normal ducts, which sometimes produce "beaded" appearance [5] (Fig. 5.3). Patients with PSC have a 10–15% lifetime risk of developing CC [11], and CC in PSC usually presents as a periductal infiltrating type CC associated with dominant stenosis [11]. Suggestive imaging findings of CC in PSC include irregular dominant stricture with a shouldered margin, prominent mural thickening, and rapidly progressed dilatation of the bile duct proximal to the stricture.

5.1.3.4 IgG4-Related Cholangitis

IgG4-related sclerosing cholangitis is the biliary manifestation of IgG4 sclerosing disease, a recently recognized disease entity that manifests histologically as infiltration by abundant IgG4-positive plasma cells [7]. Differentiation of IgG4-SC from other types of sclerosing cholangitis, espe-

Fig. 5.3 52-year-old female patient with primary sclerosing cholangitis and typical beading of the intrahepatic biliary system (arrows) as seen on coronal MRCP images. Note the normally configured extrahepatic biliary duct

cially from PSC or bile duct cancers, is clinically important as IgG4-SC shows a dramatic response to steroid therapy [12]. Unlike in PSC, multifocal strictures in IgG4-related sclerosing cholangitis are long and continuous and are associated with prestenotic dilatation. An elevated serum IgG4 level and the presence of extrabiliary IgG4 sclerosing disease (e.g., involvement of the pancreas, kidneys, thyroid gland, and salivary glands) are strongly suggestive of IgG4-related sclerosing cholangitis [7]. In cases of IgG4-SC, CT or MR imaging demonstrates long-segmental, symmetrical, circumferential wall thickening and delayed contrast enhancement of the involved bile ducts [5].

5.1.4 Neoplasms

5.1.4.1 Benign Tumors of the Bile Ducts

Common benign tumors of the bile ducts include bile duct hamartoma, adenoma, biliary papillomatosis, and biliary cystadenoma.

Biliary Hamartoma

Biliary hamartoma, also known as von Meyenburg complex, manifests as multiple or innumerable cysts, typically less than 1.5 cm, distributed in both lobes of the liver [13, 14].

Biliary Cystadenoma (Biliary Mucinous Cystic Neoplasms)

Biliary cystadenomas and cystadenocarcinomas are rare, multilocular cystic tumors of biliary origin, and more than 85% of these tumors occur in middle-aged women [15]. Biliary cystadenomas typically appear as cystic masses with a well-marginated capsule, internal septa, and mural nodules, with rare capsular calcification [14]. Although imaging features of cystadenomas and cystadenocarcinomas overlap, malignant cystadenocarcinomas tend to have a thicker wall and thicker internal septa and more often contain intratumoral papillary and polypoid projections [13].

Intraductal Papillary Neoplasm of the Bile Duct (IPNB)

Two major premalignant bile duct tumors include biliary intraepithelial neoplasia (BilIN) and intraductal papillary neoplasms of the bile duct (IPNB), both of which can progress to CC. IPNB shows a diverse spectrum of premalignant lesions toward invasive CC according to the location of the origin and presence of mucin hypersecretion. Typical imaging features of IPNB are the presence of intraductal tumors and bile duct dilatation [16]. IPNB with mucin secretion often causes dilatation of the downstream duct and patulous ampulla of Vater due to mucin hypersecretion [17]. On imaging, this can be seen as aneurysmal dilatation of the bile duct with or without visible intraductal mucin-secreting tumors, and the upstream duct can also be dilated [18, 19].

5.1.4.2 Malignant Tumors of the Bile Ducts

Cholangiocarcinoma is an adenocarcinoma arising from the bile ducts (Fig. 5.4). On the basis of macroscopic growth patterns, CC can be categorized into mass-forming (MF), periductal-infiltrating (PI), and intraductal-growing (IDG) types according to the classification proposed by the Liver Cancer Study Group of Japan (LCSGJ) [20]. Not only diagnosis of cholangiocarcinoma but also appropriate categorization of bile duct tumors based on their morphologic features and location on cross-sectional imaging studies, including computed tomography and magnetic resonance imaging, is

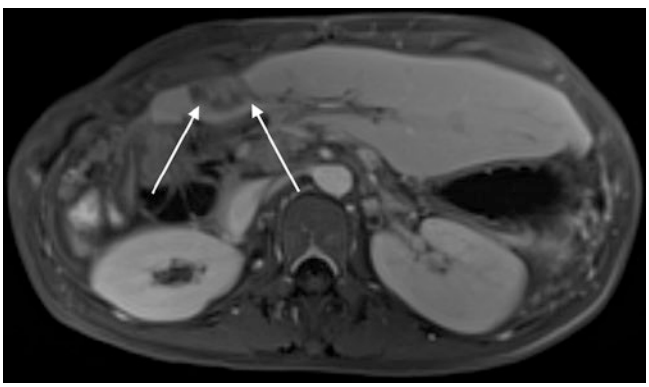

Fig. 5.4 73-year-old female patient with recurrence of cholangiocarcinoma (arrows) following right-sided hemihepatectomy with hepaticojejunal anastomosis, on equilibrium phase contrast-enhanced MR imaging

important to predict their biologic behaviors and choose relevant treatment strategies [16]. MF-type ICC typically manifests as a large non-encapsulated mass of lobulated or irregular contour, which typically shows early peripheral rim enhancement with progressive centripetal enhancement on a CT and MR imaging, and is frequently accompanied by hepatic capsular retraction and dilated peripheral bile ducts [16]. IDG-type CC appears as a polypoid or papillary tumor within the dilated bile duct lumen and has a growth pattern of superficial mucosal spreading [16].

Perihilar CC usually presents as a narrowed perihilar duct with irregular wall thickening which typically shows progressively delayed enhancement and upstream bile duct dilatation on CT or MRI [21]. Long-segmental involvement (>12 mm), a thickened (>1.5 mm) wall, luminal irregularity or asymmetry, and incremental enhancement may favor a malignant stricture, while benign strictures often involve short segments and a smooth transition [7, 22]. For perihilar cholangiocarcinomas, the local extent of the tumor is most commonly described using the Bismuth-Corlette (BC) system. Tumors are classified into type I (tumor involving only the common hepatic duct below the first confluence), type II (tumor involving the first confluence without involvement of second confluences), type III (tumor involving either right (IIIA) or left (IIIB) second confluence), and type IV (tumor involving both right and left second confluence). In general, BC type IV, BC type III with contralateral liver atrophy or contralateral vascular invasion, invasion of the main portal vein or common hepatic artery, and the presence of distant metastases are regarded to be unresectable [23]. As surgical complete resection is the only potentially curative treatment, it is critical to determine the type and extent of surgery for selection of the most appropriate surgical candidates with imaging. However, accurate staging of many CCs still remains challenging due to the small size of the tumors involved and the complex anatomy of the bile duct and adjacent structures as well as the high frequency of anatomical variations [24]. A multimodality approach using CT, MRI with MRCP, direct cholangiography, endoscopic ultrasound, and positron emission tomography has most frequently been applied to surgical candidates [24].

5.2 Gallbladder

Daniel T. Boll, M.D.

5.2.1 Normal Anatomy

Located along the undersurface of the liver in the plane of the interlobar fissure between the right and left hepatic lobes, the gallbladder is a round tubular structure with a cross-sectional diameter of up to 5 cm and a normal wall thickness of 1–3.5 mm [25, 26].

The bile-filled lumen of the gallbladder measures water isodensity (0–20 Hounsfield units) on CT and water-isointense signal characteristics on T2-weighted MR imaging; formation and retention of sludge may create gradients of signal intensity/density, resulting in a parfait-like appearance. The vicarious excretion of CT contrast material from prior contrast-enhanced CT imaging as well as utilization of hepatocyte-specific contrast materials in hepatic MR imaging may alter the imaging appearance of bile on CT as well as MR imaging [27, 28].

5.2.2 Congenital Variants and Anomalies

5.2.2.1 Agenesis of the Gallbladder

Being a rare malformation (0.01–0.2% in autopsy series), agenesis of the gallbladder results from a developmental failure of the caudal division of the primitive hepatic diverticulum or failure of vacuolization. It may result in biliary tract symptoms and formation of extrahepatic and intrahepatic gallstones in up to 50% of patients [25, 29].

5.2.2.2 Duplication of the Gallbladder

The duplication of the gallbladder is an equally rare malformation (0.02% in autopsy series), resulting in a longitudinal septum, divides the gallbladder cavity, and each cavity drains through its own cystic duct. Embryologically, duplication of the gallbladder is the result of an incomplete revacuolization of the primitive gallbladder. Differentiation from gallbladder folds, a bilobed gallbladder, a choledochal cyst, or a gallbladder diverticulum may be challenging on imaging studies [30].

5.2.2.3 Phrygian Cap of the Gallbladder

This most common anomaly of the gallbladder through a septation between the body and the distal fundus may be seen in up to 6% of all patients. Two types have been described: the retroserosal more concealed type and the serosal type with the peritoneum outlining the fundus reflecting on itself and overlying the body of the gallbladder [25, 31].

5.2.2.4 Multiseptate Gallbladder

Septations throughout the gallbladder, creating communicating chambers, may lead to stasis of bile and formation of gallstones [32].

5.2.2.5 Diverticula of the Gallbladder

True gallbladder diverticula are congenital in nature and contain all three muscle layers. Pseudodiverticula are developmental in nature and are usually associated with adenomyomatosis and contain little or no smooth muscle layers in their walls. (Pseudo)Diverticula can occur at any location throughout the gallbladder wall [25, 33].

5.2.2.6 Ectopic Gallbladder

Various locations of the gallbladder have been described; of particular interest is the intrahepatic location of the gallbladder, which is entirely surrounded by hepatic parenchyma. Intrahepatic subcapsular locations may particularly complicate the diagnosis of an acute cholecystitis as secondary signs of inflammation may be subtle or masked entirely. Shrinkage of the liver in patients with cirrhosis, as well as patients with chronic obstructive pulmonary disease, may show gallbladders interposed between the liver surface and diaphragm [25, 34].

5.2.3 Pathologic Conditions

5.2.3.1 Gallstones

The appearance of gallstones in cross-sectional imaging is primarily composition based; most gallstones contain various admixtures of bile pigment, cholesterol, and calcium. Larger proportions of calcium may render gallstones hyperdense on CT imaging, while pure cholesterol stones may be lower in CT density than surrounding bile; central inclusions of gas mostly consist of nitrogen and may lead to flotation of gallstones.

The high signal intensity of bile on T2-weighted images allows better delineation of hypointense gallstones compared to T1-weighted sequences. While cholesterol stones are usually hypointense in appearance on T1-weighted images, pigment stones tend to have higher signal intensities. Central areas of T2 hyperintensity usually corresponds to fluid-filled clefts [25, 35, 36].

5.2.3.2 Acute Cholecystitis

An obstruction of either the gallbladder neck or the cystic duct may lead to increased intraluminal pressures and eventually result in an inflammation of the gallbladder wall. Gallstones lodged in the neck of the gallbladder or the cystic duct leading to biliodynamic obstruction as well as pressure-induced mucosal ischemia and injury are the preeminent reason for acute cholecystitis. Ultrasound, CT, and MRI may show distinct features of acute cholecystitis, such as cholecystolithiasis, gallbladder wall thickening, pericholecystic fluid and inflammation, thickened bile, an indistinct interface between the gallbladder wall and liver capsule, and potentially gallbladder perforation (Fig. 5.5). Gallbladder perforations can be subdivided into acute, subacute, and chronic stages; a subacute perforation with a surrounding abscess is the most frequently encountered type of gallbladder perforation. The use of hepatobiliary contrast agents in MR imaging may provide additional functional information about cystic duct patency [25, 37, 38].

In emphysematous cholecystitis, an additional vascular compromise of the cystic artery is hypothesized to accelerate the development of gas-forming organisms in the resultant anaerobic environment with eventual penetration of gas into the gallbladder wall. A more frequent occurrence in diabetic patients, as well as the male population with an acalculous gallbladder, potentially hints at a separate pathogenesis in contrast to calculous cholecystitis [39].

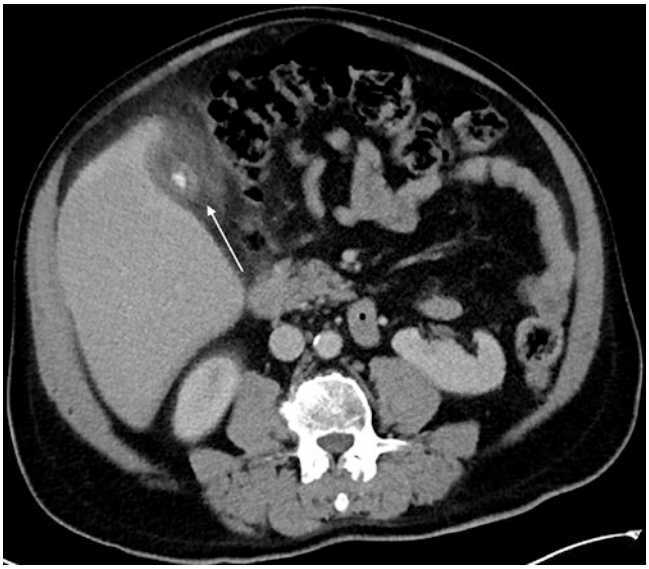

Fig. 5.5 49-year-old male patient with acute calculous cholecystitis as seen on portal venous contrast-enhanced CT imaging. Note the gallbladder wall thickening and surrounding fluid (arrow) as well as the intraluminal gallstone

Inflammation causing ulceration of the mucosal lining and subsequent necrosis may lead to hemorrhagic cholecystitis. The intraluminal hematoma that may be seen on CT and MRI may, however, be difficult to differentiate from high-intensity/high-density bile. An accompanying perforation of the gallbladder wall may lead to hemoperitoneum [40].

Coexisting cardiovascular disease predisposes patients with acute cholecystitis to develop gangrenous wall segments. Intraluminal membranes and irregularity of the gallbladder wall intermittently perforated and potentially surrounded by a pericholecystic abscess are key imaging features.

5.2.3.3 Acalculous Cholecystitis

In approximately 5% of all patients with acute cholecystitis, no intraluminal stones can be found. Long stays in intensive care units and abdominal trauma may lead to increased viscosity and subsequent stasis of bile leading to obstruction and mucosal ischemia [25, 41].

5.2.3.4 Chronic Cholecystitis

Repetitive mucosal trauma through preexisting gallstones as well as recurrent attacks of multiple acute cholecystitic episodes may contribute to the poorly understood pathogenesis of this fairly common disease. A florid inflammatory response to irritations may also indicate a genetic predisposition. While cross-sectional imaging of chronic cholecystitis may not substantially differ from acute cholecystitis, the greatest difference appears to be a contracted state of the gallbladder in chronic cholecystitis compared to the acute scenario. A decreased gallbladder ejection fraction is oftentimes associated with chronic cholecystitis [25].

Microperforations through mucosal ulcers as well as ruptured Rokitansky-Aschoff sinuses may lead to penetration of

bile into the gallbladder wall, resulting in the formation of xanthogranulomas representing the hallmark of xanthogranulomatous cholecystitis. Gallstones are almost always present, and an irregular configuration of the gallbladder wall is frequently observed. Xanthogranulomatous lesions in the wall can also lead to interim mural abscess formations. These may appear hypodense on contrast-enhanced CT imaging as well as hyperintense nodules on T2-weighted MR imaging sequences. Differentiation from gallbladder cancer may be challenging; however, a patent mucosal lining/luminal surface is more indicative of xanthogranulomatous cholecystitis [25].

Impaction of gallstones inside the cystic duct with subsequent compression of the common hepatic duct and resultant inflammation are mechanisms leading to the Mirizzi syndrome. A fairly low insertion of the cystic duct into the common hepatic duct may predispose this patient subpopulation. Differentiating the inflammatory origin of the stricture of the common hepatic duct from a neoplastic process may be challenging; the lack of lymphadenopathy, as well as a distinct focal mass, may be helpful secondary signs. Erosion of gallstones through the gallbladder wall directly into the adjacent bowel via a cholecystoenteric fistula is the most common mechanism to form a gallstone ileus, in particular within the distal ileum [25, 42].

Chronic inflammatory changes of the gallbladder wall may lead to dystrophic calcifications associated with thick fibrous tissue layers of the gallbladder wall, indicating a porcelain gallbladder. The porcelain gallbladder is frequently associated with gallbladder carcinoma [17] (Fig. 5.6).

5.2.3.5 Hyperplastic Cholecystosis

A benign proliferation of normal gallbladder wall tissue characterizes this noninflammatory condition.

A deposition of cholesterol-laden macrophages into the lamina propria of the gallbladder wall may lead to formation of cholesterol polyps and other hallmark cholesterolosis. Due to their small size, these polyps are best seen on ultrasound imaging [25, 43].

A hypertrophy of the muscular wall with corresponding mucosal overgrowth and formation of intramural diverticula and sinus tracts, then called Rokitansky-Aschoff sinuses, is the hallmark of adenomyomatosis. This disease can be seen diffusely infiltrating the gallbladder wall, may have an annular appearance, or may be very focal. Detection of a thickened gallbladder wall in addition to small cystic spaces on CT and MR imaging helps to differentiate adenomyomatosis from gallbladder cancer [43].

5.2.3.6 Gallbladder Neoplasms

Benign neoplasms of the gallbladder are rare and usually represent adenomas, which are, incidentally, (0.3–0.5%) found during cholecystectomies [25].

During the sixth or seventh decades of life with a female predilection of 2:1–3:1, gallbladder carcinomas, occur histopathologically usually as adenocarcinomas; however, adenosquamous, squamous, or neuroendocrine carcinomas can also be found, may arise from the gallbladder wall. Predisposing factors associated with gallbladder carcinoma are gallstones (75% of patients with gallbladder carcinomas have gallstones), porcelain gallbladder, genetic factors, as well as pancreaticobiliary ductal unions (reflux of pancreatic juice into the common bile duct leading to chronic inflammation) (Fig. 5.7). On cross-sectional imaging, either a mass is seen replacing the gallbladder fossa or the mass is noted filling most of the enlarged and deformed gallbladder. In invasion of surrounding structures, in particular the liver, the hepatoduodenal ligament, the right hepatic flexure, or the duodenum is frequently observed. Lymphatic spread to the regional and distant lymph nodes is very common, and gallbladder carcinoma hematogenous metastasis to the liver, intraductal tumor spread, as well as

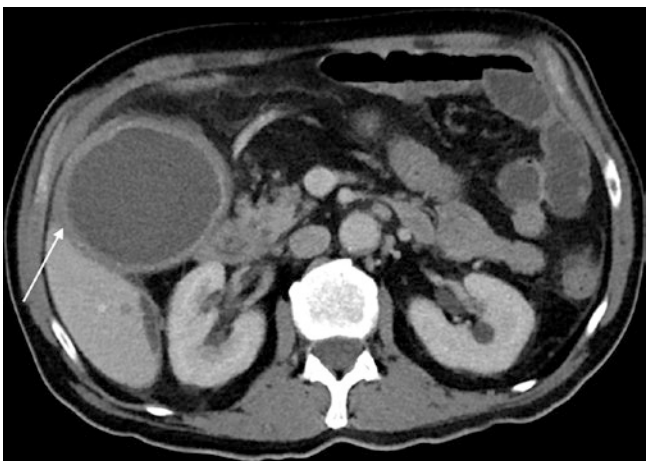

Fig. 5.6 69-year-old female patient with chronic cholecystitis with thickening of the gallbladder wall (arrow) without substantial pericholecystic fluid surrounding this acalculous gallbladder as seen on portal venous phase contrast-enhanced CT imaging

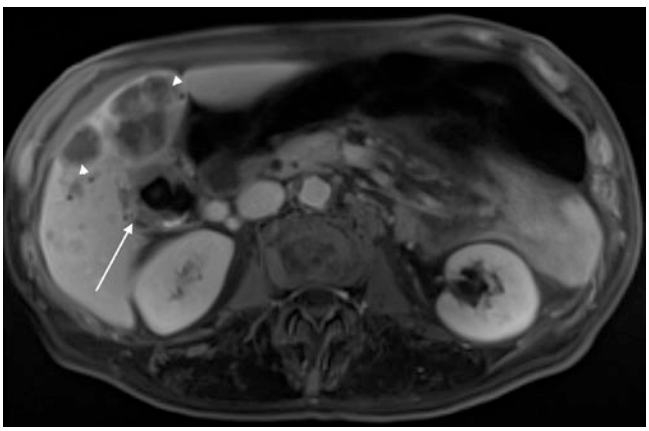

Fig. 5.7 65-year-old female patient with gallbladder carcinoma, infiltrating the liver (arrow), and multiple intrahepatic metastases (arrowheads) with gallstones on T1-weighted contrast-enhanced MR imaging using a hepatocyte-specific contrast agent in a 5-min delayed phase

peritoneal seeding is also fairly common. Biliary obstruction may be observed in up to 50% of patients [25, 44, 45].

Secondary lymphoma to the gallbladder is rare and may be seen in disseminated lymphomatous stages; primary lymphoma involving the gallbladder is extremely rare [46].

Metastases to the gallbladder is also a rare disease and can originate from any source; however, malignant melanoma is the most common cause of metastatic tumors, accounting for more than 50% of all cases of gallbladder metastases [47].

5.3 Concluding Remarks

Familiarity with the typical clinical and radiologic appearances of various etiologies of gallbladder disease, cholangiopathies, and biliary malignancies is important for accurate image interpretation, and thus enabling optimal clinical and surgical management.

Take-Home Messages

- An appreciation of the pathologic basis of gallbladder and biliary disease, combined with careful inspection of the imaging appearances, is vital for the correct interpretation of biliary studies.
- Differential diagnosis of various cholangiopathies is important because specific management exists and prognosis can be different according to the type of disease.
- Awareness of the underlying risk factors and morphologic characteristics of gallbladder disease and cholangiocarcinoma is important for accurate diagnosis and for differentiation from other hepatic tumorous and non-tumorous lesions.
- Imaging studies play important roles in the diagnosis and treatment planning of patients with biliary malignancies, and multimodality and multiparametric imaging approaches can provide complementary information in evaluating the tumor extent and resectability.

Key Points

- Imaging of gallbladder and biliary disease often requires a multimodality imaging approach.
- Sclerosing cholangitis is a spectrum of chronic progressive cholestatic liver disease characterized by inflammation, fibrosis, and stricture of the bile ducts, which can be classified as primary and secondary sclerosing cholangitis. A systematic approach combined with the appropriate clinical settings and imaging findings can be helpful for differentiating the various causes of sclerosing cholangitis.
- Although tissue biopsy or surgery is needed for the definitive diagnosis of many of biliary strictures, certain imaging characteristics of the narrowed segment (e.g., thickened wall, long-segment involvement, asymmetry, indistinct outer margin, luminal irregularity, and hyperenhancement relative to the liver parenchyma) may favor a malignant cause.
- Biliary malignancies typically demonstrate arterial phase enhancement with persistent enhancement into the portal venous phase, related to the fibrotic nature of these neoplasms.
- In the resectability assessment of perihilar CC, longitudinal tumor extent, vascular invasion, anatomical variation of the bile duct and vessels, future remnant volume, and presence or absence of distant metastasis should be considered.
- Intraductal papillary mucinous neoplasms of the bile duct (IPMN-B) bear a striking similarity to IPMN of the pancreas with regard to its histopathologic features and frequently show intraductal tumors, mucobilia, and diffuse dilatation of upstream and downstream bile ducts.
- Knowledge of congenital variants and anomalies of the gallbladder anatomy is essential to understand and characterize gallbladder disease.
- Pathogenesis of gallstone formation and resultant acute and chronic cholecystitis and their complications influences treatment decisions.
- Differentiating inflammatory gallbladder disease from gallbladder neoplasms can be challenging in early stages; recognizing imaging features which raise the suspicion for potential underlying neoplasms is essential in guiding potential treatment options.

References

1. Mortele KJ, Rocha TC, Streeter JL, Taylor AJ. Multimodality imaging of pancreatic and biliary congenital anomalies. Radiographics. 2006;26:715–31.
2. Yeh BM, Liu PS, Soto JA, Corvera CA, Hussain HK. MR imaging and CT of the biliary tract. Radiographics. 2009;29:1669–88.
3. Lee NK, Kim S, Lee JW, et al. Discrimination of suppurative cholangitis from nonsuppurative cholangitis with computed tomography (CT). Eur J Radiol. 2009;69:528–35.
4. Bader TR, Braga L, Beavers KL, Semelka RC. MR imaging findings of infectious cholangitis. Magn Reson Imaging. 2001;19:781–8.
5. Seo N, Kim SY, Lee SS, et al. Sclerosing cholangitis: Clinicopathologic features, imaging Spectrum, and systemic approach to differential diagnosis. Korean J Radiol. 2016;17:25–38.
6. Heffernan EJ, Geoghegan T, Munk PL, Ho SG, Harris AC. Recurrent pyogenic cholangitis: from imaging to intervention. AJR Am J Roentgenol. 2009;192:W28–35.
7. Katabathina VS, Dasyam AK, Dasyam N, Hosseinzadeh K. Adult bile duct strictures: role of MR imaging and MR cholangiopancreatography in characterization. Radiographics. 2014;34:565–86.

8. Kim JH, Kim TK, Eun HW, et al. CT findings of cholangiocarcinoma associated with recurrent pyogenic cholangitis. AJR Am J Roentgenol. 2006;187:1571–7.
9. Al-Sukhni W, Gallinger S, Pratzer A, et al. Recurrent pyogenic cholangitis with hepatolithiasis--the role of surgical therapy in North America. J Gastrointest Surg. 2008;12:496–503.
10. Eaton JE, Talwalkar JA, Lazaridis KN, Gores GJ, Lindor KD. Pathogenesis of primary sclerosing cholangitis and advances in diagnosis and management. Gastroenterology. 2013;145:521–36.
11. Khaderi SA, Sussman NL. Screening for malignancy in primary sclerosing cholangitis (PSC). Curr Gastroenterol Rep. 2015;17:17.
12. Ponsioen CY. Diagnosis, differential diagnosis, and epidemiology of primary Sclerosing cholangitis. Dig Dis. 2015;33(Suppl 2):134–9.
13. Buetow PC, Midkiff RB. MR imaging of the liver. Primary malignant neoplasms in the adult. Magn Reson Imaging Clin N Am. 1997;5:289–318.
14. Yam BL, Siegelman ES. MR imaging of the biliary system. Radiol Clin N Am. 2014;52:725–55.
15. Devaney K, Goodman ZD, Ishak KG. Hepatobiliary cystadenoma and cystadenocarcinoma. A light microscopic and immunohistochemical study of 70 patients. Am J Surg Pathol. 1994;18:1078–91.
16. Joo I, Lee JM. Imaging bile duct tumors: pathologic concepts, classification, and early tumor detection. Abdom Imaging. 2013;38:1334–50.
17. Kane RA, Jacobs R, Katz J, Costello P. Porcelain gallbladder: ultrasound and CT appearance. Radiology. 1984;152:137–41.
18. Lim JH, Yoon KH, Kim SH, et al. Intraductal papillary mucinous tumor of the bile ducts. Radiographics. 2004;24:53–66.
19. Takanami K, Yamada T, Tsuda M, et al. Intraductal papillary mucininous neoplasm of the bile ducts: multimodality assessment with pathologic correlation. Abdom Imaging. 2011;36:447–56.
20. Yamasaki S. Intrahepatic cholangiocarcinoma: macroscopic type and stage classification. J Hepato-Biliary-Pancreat Surg. 2003;10:288–91.
21. Valls C, Ruiz S, Martinez L, Leiva D. Radiological diagnosis and staging of hilar cholangiocarcinoma. World J Gastrointest Oncol. 2013;5:115–26.
22. Kim JY, Lee JM, Han JK, et al. Contrast-enhanced MRI combined with MR cholangiopancreatography for the evaluation of patients with biliary strictures: differentiation of malignant from benign bile duct strictures. J Magn Reson Imaging. 2007;26:304–12.
23. Jarnagin WR, Fong Y, DeMatteo RP, et al. Staging, resectability, and outcome in 225 patients with hilar cholangiocarcinoma. Ann Surg. 2001;234:507–17.
24. Corona-Villalobos CP, Pawlik TM, Kamel IR. Imaging of the patient with a biliary tract or primary liver tumor. Surg Oncol Clin N Am. 2014;23:189–206.
25. Lim JH, Kim KW, Choi D-i. Biliary tract and gallbladder. In: Haaga JR, Boll DT, editors. CT and MRI of the whole body. 6th ed. Philadelphia: Elsevier; 2017. p. 1192–267.
26. Smathers RL, Lee JK, Heiken JP. Differentiation of complicated cholecystitis from gallbladder carcinoma by computed tomography. AJR Am J Roentgenol. 1984;143:255–9.
27. Havrilla TR, Reich NE, Haaga JR, Seidelmann FE, Cooperman AM, Alfidi RJ. Computed tomography of the gallbladder. AJR Am J Roentgenol. 1978;130:1059–67.
28. Strax R, Toombs BD, Kam J, Rauschkolb EN, Patel S, Sandler CM. Gallbladder enhancement following angiography: a normal CT finding. J Comput Assist Tomogr. 1982;6:766–8.
29. Al-Fallouji MA. Perforated posterior peptic ulcer associated with gallbladder agenesis and midgut malrotation. Br J Clin Pract. 1983;37:353–6. 358
30. Udelsman R, Sugarbaker PH. Congenital duplication of the gallbladder associated with an anomalous right hepatic artery. Am J Surg. 1985;149:812–5.
31. Foster DR. Triple gall bladder. Br J Radiol. 1981;54:817–8.
32. Toombs BD, Foucar E, Rowlands BJ, Strax R. Multiseptate gallbladder. South Med J. 1982;75:610–2.
33. Kochhar R, Nagi B, Mehta SK, Gupta NM. ERCP diagnosis of a gallbladder diverticulum. Gastrointest Endosc. 1988;34:150–1.
34. Gore RM, Ghahremani GG, Joseph AE, Nemcek AA Jr, Marn CS, Vogelzang RL. Acquired malposition of the colon and gallbladder in patients with cirrhosis: CT findings and clinical implications. Radiology. 1989;171:739–42.
35. Brink JA, Ferrucci JT. Use of CT for predicting gallstone composition: a dissenting view. Radiology. 1991;178:633–4.
36. Tsai HM, Lin XZ, Chen CY, Lin PW, Lin JC. MRI of gallstones with different compositions. AJR Am J Roentgenol. 2004;182:1513–9.
37. Bennett GL, Balthazar EJ. Ultrasound and CT evaluation of emergent gallbladder pathology. Radiol Clin N Am. 2003;41:1203–16.
38. Paulson EK. Acute cholecystitis: CT findings. Semin Ultrasound CT MR. 2000;21:56–63.
39. Jacob H, Appelman R, Stein HD. Emphysematous cholecystitis. Am J Gastroenterol. 1979;71:325–30.
40. Jenkins M, Golding RH, Cooperberg PL. Sonography and computed tomography of hemorrhagic cholecystitis. AJR Am J Roentgenol. 1983;140:1197–8.
41. Mirvis SE, Vainright JR, Nelson AW, et al. The diagnosis of acute acalculous cholecystitis: a comparison of sonography, scintigraphy, and CT. AJR Am J Roentgenol. 1986;147:1171–5.
42. Koehler RE, Melson GL, Lee JK, Long J. Common hepatic duct obstruction by cystic duct stone: Mirizzi syndrome. AJR Am J Roentgenol. 1979;132:1007–9.
43. JUTRAS JA. Hyperplastic cholecystoses; hickey lecture, 1960. Am J Roentgenol Radium Therapy, Nucl Med. 1960;83:795–827.
44. Hamrick RE Jr, Liner FJ, Hastings PR, Cohn I Jr. Primary carcinoma of the gallbladder. Ann Surg. 1982;195:270–3.
45. Yoshimitsu K, Honda H, Shinozaki K, et al. Helical CT of the local spread of carcinoma of the gallbladder: evaluation according to the TNM system in patients who underwent surgical resection. AJR Am J Roentgenol. 2002;179:423–8.
46. Mitropoulos FA, Angelopoulou MK, Siakantaris MP, et al. Primary non-Hodgkin's lymphoma of the gall bladder. Leuk Lymphoma. 2000;40:123–31.
47. Guida M, Cramarossa A, Gentile A, et al. Metastatic malignant melanoma of the gallbladder: a case report and review of the literature. Melanoma Res. 2002;12:619–25.